Cuboid Based Novel Simulation Using SAXS for Enhanced Roughness Metrology

1st Nischal Dhungana
CEA-Leti, Univ. Grenoble Alpes
F-38000 Grenoble, France
nischal.dhungana@cea.fr

2nd Guillaume Freychet
CEA-Leti, Univ. Grenoble Alpes
F-38000 Grenoble, France

3rd Tristan Dewolf
CEA-Leti, Univ. Grenoble Alpes
F-38000 Grenoble, France

4th Matteo Knebel
CEA-Leti, Univ. Grenoble Alpes
F-38000 Grenoble, France

5th Patrice Gergaud
CEA-Leti, Univ. Grenoble Alpes
F-38000 Grenoble, France

***Abstract*—The relentless scaling of semiconductor features demands ever-greater precision in roughness characterization. Here, we introduce an analytical SAXS simulation for periodic transmission gratings that models line-edge roughness (LER) by laterally shifting cuboid centers and line-width roughness (LWR) via width modulation of each cuboid in a finite stack. By summing the individual sinc form factors, we derive closed-form diffraction intensities and compute the power spectral density (PSD) directly in Fourier space, bypassing image discretization. A vectorized implementation accelerates PSD extraction by over two orders of magnitude compared to binary-FFT methods, while accurately recovering the roughness parameters: root mean square σ, correlation length ξ, and Hurst exponent α. This framework offers a rapid, non-destructive route to high-fidelity roughness metrology for next-generation lithographic structures.**

***Index Terms*—Roughness Characterization, Power Spectral Density (PSD), Small Angle X-ray Scattering (SAXS)**

I. Introduction

The continued scaling of semiconductor devices into smaller and smaller nodes requires more sensitive and accurate techniques for roughness characterization. Currently, methods such as Critical Dimension Scanning Electron Microscopy (CD-SEM) and Atomic Force Microscopy (AFM) are widely used [1]. In these techniques, images of the nanostructure are first acquired, and the roughness profile is then extracted algorithmically. Acquiring many images allows for the selection of statistically significant profiles. This profile is typically characterized in the frequency domain by computing the power spectral density (PSD) (see figure 2) of the roughness [5]. The PSD is defined as the squared magnitude of the Fourier transform of the surface height (or edge) fluctuations, and it provides a statistical representation of how roughness is distributed over spatial frequencies.

Two kinds of roughness are often considered in these methods: Line Edge Roughness (LER) and Line Width Roughness (LWR), as illustrated in figure 1.

(Part of) This work, carried out on the Platform for Nanocharacterisation (PFNC), was supported by the "Recherche Technologique de Base" and "France 2030 - ANR-22-PEEL-0014" programs of the French National Research Agency (ANR).

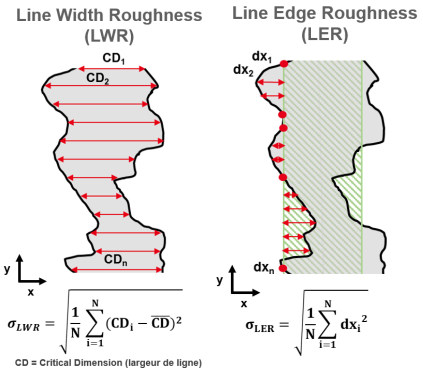

(a) (b)

Fig. 1: a) LWR representation where the 3σ variation is in the measured width of the line. b) LER roughness of a line, measured as a 3σ deviation from a reference straight edge. [2]

Crucial roughness parameters—including the roughness amplitude's standard deviation (σ), the correlation length (ξ), and the Hurst exponent (α)—can be determined from the PSD when it is extracted along the relevant spatial direction [2], [4].

An attractive alternative to the CDSEM/AFM imaging methods is offered by X-ray based techniques, notably Critical Dimension Small Angle X-ray Scattering (CD-SAXS). Unlike imaging methods, CD-SAXS measurements provide direct access to the Fourier space (diffraction patterns) of the rough nanostructure. We can directly access the frequency domain and thus the PSD without the intermediate step of image processing. [3]. However, extracting accurate roughness parameters from CD-SAXS remains challenging, as the signal arising from surface roughness is often convoluted with other structural features of the nanostructure.

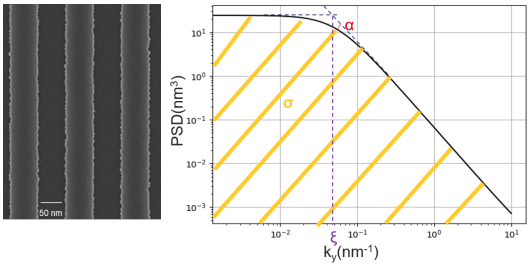

(a) (b)

Fig. 2: a) Top view CD-SEM image with the red line indicating the extracted roughness profile. b) Representation of power spectral density (PSD) that can be derived from the profile. It is used to extract the characterization parameters: σ, α, and ξ.

II. Previous Work

Reche et al. demonstrated that CD-SAXS measurements can be used to extract roughness information from line gratings [3]. Their simulation approach involves generating a binary image of the grating and applying a fast Fourier transform to compute the PSD at points where Bragg's diffraction spots are extinct (shown by a blue arrow in figure 3b). While conceptually straightforward, this approach has few limitations. The binary projection oversimplifies the inherently three-dimensional nature of roughness, and the extracted PSD is susceptible to resolution limits and discretization artifacts. Moreover, if the pixel size is relatively large compared to the small, fractional variations of the roughness, critical details may be lost. To capture these nuances accurately, a smaller pixel size is required, which can be computationally expensive.

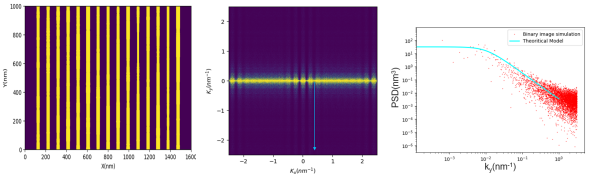

(a) (b) (c)

Fig. 3: a) Representation of line gratings and its roughness in a binary image as used in simulations by Reche et al. b) Fourier transform of the binary image. The blue arrow represent an extinction point where the PSD can be extracted. c) PSD obtained from the average of ten Fourier transforms as presented in b).

III. Analytical Model

To address the limitations of earlier approaches, an analytical model was conceived. It simulates diffraction from a periodic line structure incorporating both line edge roughness (LER) and line-width roughness (LWR). Each line is composed of a stack of N identical cuboids ("cubes") of width a, height b, and depth Δy. For LWR, the cuboid widths are modulated by the roughness profile, and for LER each cuboid is laterally shifted by the corresponding roughness deviation. (see figure 4).

The Form factor of a single cuboid then can be written as:

$$F_{\text{cube}}(k_x, k_y, k_z) = sinc\left(\frac{a k_x}{2}\right)\ sinc\left(\frac{\Delta y\, k_y}{2}\right)\ sinc\left(\frac{b k_z}{2}\right). \tag{1}$$

Fourier transform for the case of LER then becomes:

$$F_{\text{stack}}(\mathbf{k}) = F_{\text{cube}}(a, b, \Delta y) \sum_{n=0}^{N-1} e^{-i\left[k_y\, n\, \Delta y + k_x\, \omega_n\right]}, \tag{2}$$

where $\{\omega_n\}_{n=0}^{N-1}$ denotes a set of a stationary Gaussian roughness profile.

In the case of LWR,

$$F_{\text{stack}}(\mathbf{k}) = \sum_{n=0}^{N-1} F_{\text{cube}}\left(a, b, \Delta y + \omega_n\right) e^{-i\, k_y\, n\, \Delta y}. \tag{3}$$

By summing the individual form factors, shifted or resized according to the prescribed roughness profile, we obtain the diffraction pattern of the grating (Fig. 5).

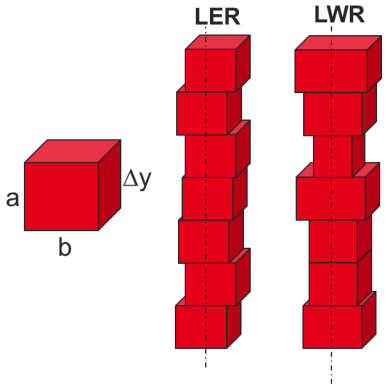

Fig. 4: Cuboid model illustrating LER as shifts in the centers of cuboids and LWR as variations in their widths.

A vertical cut through the extinction point of the resulting diffraction image (shown in figure 5a) yields the PSD, analogous to the binary-image method. This analytical framework affords precise control over simulation parameters, such as resolution and spatial extent, so that in figure 5a we present a zoomed-in view over a narrow range of k_x and k_y, in contrast to figure 3b. Such flexibility enables a tailored trade-off between accuracy and computational cost. By choosing a resolution sufficient to capture essential features without unnecessary overhead, diffraction-image generation can be accelerated by up to two orders of magnitude, making PSD simulation both faster and more robust.

As shown in figure 5b, the analytical cuboid model exhibits smaller deviations from the theoretical PSD and produces fewer artifacts than the binary-image approach under identical conditions (see figure 3).

Despite its advantages in speed and reliability, this technique cannot overcome all limitations of prior method. PSD analysis remains confined to extinction points since elsewhere

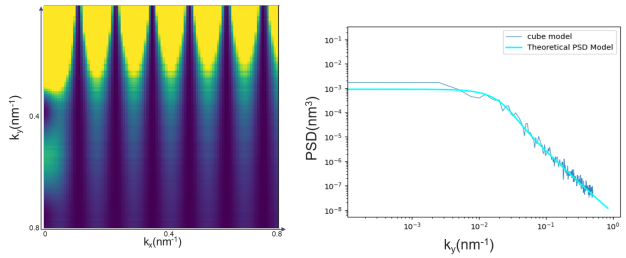

(a) (b)

Fig. 5: a) Fourier transform of the LER analytical model with extinction points indicated. b) PSD obtained by averaging the Fourier transforms of ten lines at these points.

the signal is convoluted with other scattering components. Similarly, accurate extraction of the roughness amplitude σ remains challenging. Indeed, the damping-factor approach of Herrero et al. [6] offers a theoretical path to σ, although obtaining all the necessary experimental inputs with adequate precision can be difficult.

While testing this technique, we observed that the PSD signature is present across the entire diffraction pattern but is heavily masked by the grating-structure signal, making it visible only at the extinction points. This limitation motivated us to develop a theoretical model for cube diffraction, which will deepen our understanding of the various features in the diffraction image and ultimately enable us to deconvolute the PSD contribution more effectively.

IV. Theoretical Modelling

We reviewed related formulations in the literature and found that the work of Sinha et al. [7], which treats X-ray reflectivity from surfaces with Gaussian roughness. It parallels our problem of transmission through line gratings. We therefore adopted and adapted Sinha's derivation to develop a more accurate theoretical framework for our system.

Sinha *et al.* split the scattering cross section $S(k_x, k_y)$ in the first-Born approximation into a specular (coherent) ridge and a diffuse term,

$$S_{\text{spec}}(k_x, k_y) = e^{-k_x^2\sigma^2}\,\delta(k_x)\,\delta(k_y), \tag{4}$$

$$S_{\text{diff}}(k_x, k_y) = 2\,e^{-k_x^2\sigma^2}\int_0^L (L-r)\,R_W(r)\,J_0(k_y\,r)\,dr, \tag{5}$$

where J_0 is the zeroth-order Bessel function.

We made the following further simplifying assumptions for the case of LER to observe the PSD directly in the expression:

1) The lateral shifts $\{\omega_n\}$ form a zero-mean, stationary Gaussian process:
$$\langle \omega_n \rangle = 0$$
2) Either the roughness amplitude or k_x is small enough that $k_x^2\,R_W(0) = k_x^2\,\sigma^2 \ll 1$, where $R_W(r) = \langle \omega(y)\,\omega(y+r)\rangle$ is the covariance function.
3) The stack is sufficiently tall that boundary effects other than the finite lateral length may be neglected.

Under these conditions, one obtains after Gaussian averaging the finite-L intensity:

$$\langle I(\mathbf{k})\rangle \propto \left|F_{\text{cube}}(\mathbf{k})\right|^2 e^{-k_x^2\sigma^2}\int_{-L}^{L}(L-|r|)\,e^{-ik_y r}\left[1+k_x^2 R_W(r)\right]dr, \tag{6}$$

and we obtain the following approximation form for LER:

$$\langle I(\mathbf{k})\rangle \propto |F_{\text{cube}}(\mathbf{k})|^2\,e^{-k_x^2 R_\omega(0)} \times\left[\frac{2\left[1-\cos(k_y L)\right]}{k_y^2} + L\cdot k_x^2\,S_W(k_y)\right], \tag{7}$$

where $S_W(k_y)$ is the power spectral density (PSD).

Let's now compare Sinha's results to ours:

1) **Coherent/specular ridge.**
In our model, the integral
$$\int_{-L}^{L}(L-|r|)\,e^{-ik_y r}\,dr = \frac{2[1-\cos(k_y L)]}{k_y^2}$$
sharpens to a Dirac delta peak, $\delta(k_y)$, as $L\to\infty$. Likewise, Sinha's S_{spec} in Eq. (4) contains $\delta(k_y)\,\delta(k_x)$, representing perfect specular reflection.
2) **Debye–Waller damping.**
Both treatments feature the Gaussian prefactor $e^{-k_x^2\sigma^2}$, which uniformly attenuates all coherent and diffuse scattering orders, analogous to the Debye–Waller factor observed in the paper by Herrero *et al.* [6].
3) **Diffuse component.**
Our additional term
$$k_x^2\int_{-L}^{L}(L-|r|)\,R_W(r)\,e^{-ik_y r}\,dr \approx L\cdot k_x^2\,S_W(k_y)$$
generates off-specular sidebands around each extinction point. This mirrors Sinha's diffuse intensity in Eq. (5), and is the term that contains the PSD under our approximations.

By aligning each mathematical structure and damping mechanism, we see that our finite-stack cuboid model recovers exactly the same specular and diffuse behavior that Sinha's Born approximation predicts for a rough surface, but expressed here in the language of periodic line gratings in transmission.

We can now leverage our theoretical framework to predict the simulated diffraction pattern with high accuracy. Crucially, this approach enables us to recover the input PSD and the three roughness characterization parameters more accurately from the simulations. In figure 6, the prediction of Eq. (6) is compared against the numerically simulated results from the previous method, and the two curves align well.

The simulated intensity was subsequently processed by isolating only the PSD contribution at a non-extinction point. The resulting PSD, presented in figure 7, closely reproduces the input spectrum used to generate the simulation. This agreement indicates that, within the framework of our approximations,

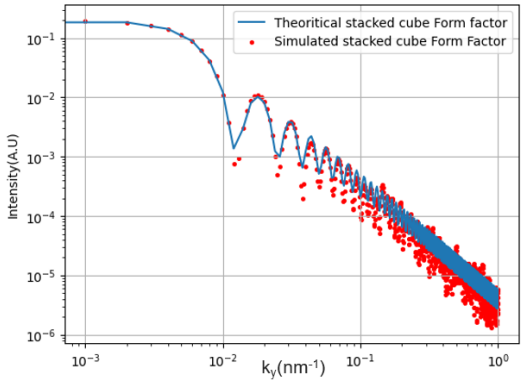

Fig. 6: Comparison between the analytical prediction of Eq. (6) (blue line) and the numerically simulated diffraction intensity (dots) at a non-extinction point. The overlap demonstrates the model reliably predicts the numerical simulation.

it is possible to extract the PSD away from the extinction conditions typically required by earlier methods.

Nonetheless, a residual noise floor remains visible in figure 7. We attribute this artifact to the simplifying assumptions inherent in our model. Relaxing some of these approximations in future work may enhance fidelity and reduce the background signal. In addition, normalization remains an issue; a thorough derivation and estimation of the normalization constant will be necessary. Finally, applying this theoretical framework to LWR modelling is a key objective for future work.

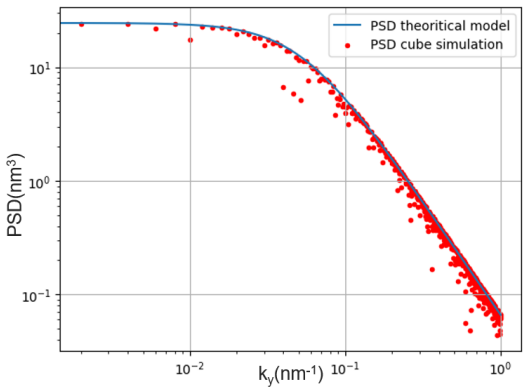

Fig. 7: Recovered power spectral density at a non-extinction point (red dots), overlaid with the input PSD used to generate the simulation (blue line). The close agreement verifies the ability of our method to extract the PSD outside extinction conditions, while the residual noise floor reflects the limitations of the simplifying assumptions.

V. Conclusion and Perspectives

In this work, we have developed an analytical diffraction-based method for direct extraction of the PSD of line-edge roughness (LER) in periodic transmission gratings. Specifically, by adapting Sinha *et al.*'s Born-approximation treatment of Gaussian surface roughness to a finite-stack cuboid model, we derived closed-form expressions for both the coherent (specular) and diffuse scattering contributions [Eqs. (6)–(7)]. Comparison with numerical simulations demonstrates that our framework recovers the input PSD and the three key roughness parameters σ, correlation length ξ, and Hurst exponent α, even away from extinction points, thus extending PSD extraction beyond the extinction only limitations of previous approaches.

The next step is to measure transmission-grating samples at a synchrotron to capture the high-flux, low-background off-specular signal required to validate our theoretical predictions under realistic scattering conditions. Following initial validation, we will extend the protocol to nanostructured samples—high-aspect-ratio lines, multilayer stacks, and patterned wafers—to test its robustness against real-world fabrication non-idealities.

Benchmarking against state-of-the-art metrology is essential. We will perform a head-to-head comparison of our diffraction-based PSD extraction with critical-dimension scanning electron microscopy (CD-SEM) and critical-dimension atomic force microscopy (AFM), evaluating not only accuracy in the determination of σ, ξ, and α but also spatial-frequency coverage, throughput, and sensitivity to noise or imaging artifacts.

Through these experimental tests, comparative benchmarks, and further theoretical refinements, we aim to establish X-ray diffraction–based roughness metrology as a rapid, non-destructive, and statistically robust complement to CD-SEM and AFM for next-generation semiconductor manufacturing.

References

[1] Kizu, R., Misumi, I., Hirai, A., and Gonda, S., "Direct comparison of line edge roughness measurements by SEM and a metrological tilting-atomic force microscopy for reference metrology," *J. Micro/Nanolithography, MEMS, and MOEMS*, vol. 19, no. 4, p. 044001, 2020. doi:10.1117/1.JMM.19.4.044001. [Online]. Available: https://doi.org/10.1117/1.JMM.19.4.044001.

[2] Reche, J., *Nouvelle méthodologie hybride pour la mesure de rugosités sub-nanométriques* (Ph.D. thesis), Université Grenoble Alpes, 2019. [Online]. Available: https://theses.hal.science/tel-02520554.

[3] Reche, J., Gergaud, P., Blancquaert, Y., Besacier, M., and Freychet, G., "Shape and Roughness Extraction of Line Gratings by Small Angle X-Ray Scattering: Statistics and Simulations," *IEEE Trans. Semicond. Manuf.*, vol. 35, no. 3, pp. 425–431, 2022. doi:10.1109/TSM.2022.3176026.

[4] Moussa, A., Lorusso, G., Sutani, T., Rutigliani, V., Roey, F., Mack, C., Naulleau, P., Constantoudis, V., Ikota, M., Ishimoto, T., and Koshihara, S., "The need for line-edge roughness metrology standardization: the imec protocol (Conference Presentation)," in *Proc. SPIE*, Mar. 2018, p. 12. doi:10.1117/12.2294617.

[5] Azar-Nouche, L., "Défis liés à la réduction de la rugosité des motifs de résine photosensible 193 nm" (Ph.D. thesis, Université de Grenoble, 2012). [Online]. Available: https://theses.hal.science/tel-00767820.

[6] Analía Fernández Herrero, Mika Pflüger, Jürgen Probst, Frank Scholze, and Victor Soltwisch, "Applicability of the Debye-Waller damping factor for the determination of the line-edge roughness of lamellar gratings," Opt. Express 27, 32490-32507 (2019) https://opg.optica.org/oe/fulltext.cfm?uri=oe-27-22-32490&id=422573,

[7] Sinha, Sunil and Sirota, E. and Garoff, S and Stanley, Halina, 1988,X-Ray and Neutron Scattering from Rough Surfaces journal:Physical review. B, Condensed matter doi:10.1103/PhysRevB.38.2297